Experimental study on the evolution of canyon fire spread behavior under different terrains and the critical conditions for eruptive fire

Jiale Fan^A, Boxuan Chen^A, Yan Guo^A, Chenze Bu^A, Jiangxue Gao^A, Xu Dou^A, Haiging Hu^A, Long Sun^{A,*} and Tongxin Hu^{A,*}

For full list of author affiliations and declarations see end of paper

*Correspondence to:

Long Sun Key Laboratory of Sustainable Forest Ecosystem Management - Ministry of Education, Northern Forest Fire Management Key Laboratory of State Forestry and Grassland Administration, College of Forestry, Northeast Forestry University, 26 Hexing Road, Harbin 150040,

Email: sunlong365@126.com

Key Laboratory of Sustainable Forest Ecosystem Management - Ministry of Education, Northern Forest Fire Management Key Laboratory of State Forestry and Grassland Administration, College of Forestry, Northeast Forestry University, 26 Hexing Road, Harbin 150040,

Email: htxhtxapple@sina.com

Received: 14 August 2024 Accepted: 15 September 2025 Published: 13 October 2025

Cite this: Fan J et al. (2025) Experimental study on the evolution of canyon fire spread behavior under different terrains and the critical conditions for eruptive fire. International Journal of Wildland Fire 34, WF24134. doi:10.1071/WF24134

© 2025 The Author(s) (or their employer(s)). Published by CSIRO Publishing on behalf of IAWF.

This is an open access article distributed under the Creative Commons Attribution-NonCommercial-NoDerivatives 4.0 International License (CC BY-NC-ND)

OPEN ACCESS

ABSTRACT

Background. The spread of canyon fire often involves sudden acceleration, which is related to eruptive fire. Aims. The purpose of the study is to explore the pattern of fire line evolution and rate of spread (ROS) with topographic conditions in canyon fire, and to clarify the critical conditions for and mechanism of eruptive fire. Methods. A systematic experimental study on canyon fire was conducted by igniting dead pine needles with a point ignition. Key results. Four different types of fire line contours were identified under different topographic conditions. When the central slope angle $\alpha \ge 15^\circ$, the direction of the fire head gradually deviates from the line of maximum slope and moves to the center line, and this deviation increases with α . Accordingly, ROS along the center line also exhibits dynamic characteristics, and ROS increases with α and the lateral slope angle δ . The critical conditions for eruptive fire are α = 27.5° and δ = 20°. Conclusions. When eruptive fire occurs, there is significant convective heating ahead of the fire front. This strong convective heating is the basic mechanism for eruptive fire in canyons. Implications. Our results may provide a theoretical basis to assist fire commanders to make decisions.

Keywords: canyon fire, convective heating, critical conditions, eruptive fire, extreme fire behavior, fire front, fire line contour, rate of spread, terrain.

Introduction

In recent years, global changes dominated by climate change have contributed to more flammable landscapes and unstable atmospheric conditions, promoting the development of wildfires, with extreme fire behaviors becoming more frequent (Viegas et al. 2009; Duane et al. 2021; Wadhwani et al. 2023). Extreme fire behavior is seen when fires undergo an unsteady physical transition from the original low-intensity steady state to a new steady state with a high rate of spread (ROS) and intensity (Liu 2023). Eruptive fire is a typical extreme fire behavior and is also referred to as 'blow-up', 'flashover', or 'fire eruption' (Liu et al. 2021). It is characterized by a sharp increase in the ROS and heat release rate in a very short time, regardless of changes in the external environmental conditions (Viegas 2004; Liu et al. 2021). This sudden and unpredictable change in fire behavior is very dangerous for firefighters, with many casualties being related to it (Viegas and Pita 2004; Viegas et al. 2009; Chatelon et al. 2011; Xie et al. 2017). Previous cases and studies indicate that eruptive fire is likely to occur on steep slopes, such as canyons or ridges (Viegas 2004; Viegas and Simeoni 2011; Viegas et al. 2021a). The control mechanism of extreme fire behavior is completely different from that of general steady-state surface fire, and we still do not fully understand it, which is one of the causes of such accidents (Liu et al. 2023; Wadhwani et al. 2023).

Some progress has been made in research on eruptive fire behavior and its acceleration mechanism. Viegas and Pita (2004) put forward a groundbreaking explanation that under the conditions of a downwind or positive slope, fire eruption may be caused by the convective heat feedback effect induced by the fire front. The flow induced by fire provides fresh oxygen to the reaction zone, enhancing the combustion process and

resulting in an increase in ROS and flame length, simultaneously leading to flame entrainment of more ambient air and further increasing ROS (Silvani et al. 2012, 2018; Liu et al. 2014). If this positive feedback process is not suppressed, ROS will continue to increase, possibly reaching very high values (Viegas and Simeoni 2011). Dold and Zinoviev (2009) proposed that flow attachment to the fuel surface is the key factor leading to the acceleration of fire spread on the confined slope ahead of the fire front. They erected two 60-cm baffles on either side of an inclined fuel bed to prevent lateral airflow, which was used as an analogy for a narrow canyon. The airflow ahead of the fire front was observed approximately through soap bubbles injected into the air. The results showed that flow attachment occurs at a larger slope angle, accelerating fire spread. However, there was no quantitative measurement to study the relationship between flow attachment and fire spread acceleration from a physical layer. Xie et al. (2017) conducted a systematic experimental study on upslope fire spread in a trench. The experiments showed that flow attachment is the result of the combined effect of slope and trench structure on air entrainment limitation. When flow attachment occurs, convective heating is enhanced, and the range of its influence considerably increases, with this becoming an important mechanism for fuel preheating Liu et al. (2023) studied fire spread characteristics and the critical conditions of fire in different trench structures and found that compared with radiative heating, convective heating caused by flow attachment plays a more critical role in fire spread. For a given terrain slope, when the aspect ratio of the trench increased to a certain value, it had no effect on eruptive fire behavior, indicating a ceiling effect.

Canyon fires exhibit considerably different fire line evolution and fire spread behaviors compared with normal upslope fires (Xie et al. 2020). Upslope fire can rapidly reach a steady state, with a constant ROS after ignition. Most previously developed fire spread models are also based on this 'quasisteady state' hypothesis (Rothermel 1972; Viegas 2006; Chatelon et al. 2011; Dold and Zinoviev et al. 2011; Balbi et al. 2014). Owing to complex terrain or other reasons, the ROS of canyon fires exhibits dynamic characteristics, making it difficult to reach a stable state in a short time. Fire eruptions may occur on steep slopes, causing the ROS to increase sharply (Viegas and Pita 2004; Xie et al. 2020). However, research directly related to canyon fire is very limited. Lopes et al. (1995) are the pioneers of the study of fire spread in canyons, using a complete physical equation to numerically simulate the canyon fire spread process, proving the acceleration of airflow in the canyon and the influence of wind-fire interaction on fire behavior. Viegas and Pita (2004) conducted further research on canyon fire, proposed a simple analysis model and conducted a series of laboratory experiments on a symmetric canyon. The purpose of the model was only as a reference, without considering the interaction between adjacent fire lines in the canyon. The results showed that only

under conditions of low central slope angle α and high lateral slope angle δ can an obvious bifurcated fire head be observed. In most other cases, the fire front on the center line tends to catch up with the other two heads and merge into a single and broad fire front. As the slope increases, the direction of the fire head deviates from the line of maximum slope and gradually moves to the center line. When $\alpha = 20^{\circ}$ and δ is $>20^{\circ}$, the ROS along the central line shows dynamic characteristics; when α is $\geq 30^{\circ}$, the ROS index increases and an eruptive fire occurs. The authors believe this fire spread acceleration is caused by fire-induced flow. However, there was no quantitative measurement of flow velocity and heat flux density to explore the heat transfer mode ahead of the fire front. Building on Viegas' study, Xie et al. (2020) explored the spread process and heat transfer mechanism of canyon fire through experimental research and theoretical analysis. The results showed that under distinct α conditions, there are three different fire line evolution modes, which lead to different ROS change modes along the central line. The experimentally measured convection heat flux, velocity and calculated convection heat transfer confirmed that when α reaches the critical angle, an eruptive fire occurs, and there is obvious convective heating ahead of the fire front, which is caused by the significant interaction between the two lateral fire fronts in the canyon. This convective heating effect is considered a potential mechanism for eruptive fire in a canyon. However, the study only changed the central slope angle and did not consider the influence of the side slope angle. Pimont et al. (2012) conducted a numerical simulation of a canyon fire. The results showed that in downwind conditions, the ROS in a narrow canyon was slightly higher than in a wide canyon. The ROS was significantly affected by the combined effects of wind, slope and fire front size. Additionally, Viegas et al. (2021a) conducted a laboratory-scale study on linear fire entering transverse canyons perpendicular to the main fire spread direction, whereas Rodrigues et al. (2023) studied the spread of linear fire on slopes embedded in canyons. These studies showed that the special terrain configuration of canvons can lead to changes in fire spread behavior, leading to accelerated fire spread and fire eruption under certain conditions. However, there is no systematic analysis of the influence of canyon shape on fire line evolution and ROS, and the critical conditions for the occurrence of eruptive fire in canvons remain unclear.

Herein, we conducted a series of experiments on canyon fire spread under different terrain conditions on a pine needle fuel bed. We systematically analyzed the changing pattern of the fire line evolution and ROS in the canyon with terrain slope and explored the critical conditions for eruptive fire. By measuring the heat flux and flow velocity of the fire front, we analyzed the preheating mechanism under different conditions, its relationship with the acceleration of fire spread and the influence of terrain on convective heat transfer. The results further deepen understanding of canyon fire behavior, lay a foundation for the establishment of a

canyon fire prediction model and provide a scientific basis for firefighting commanders.

Materials and methods

Geometric structure of the canyon

The geometric structure of the symmetrical canyon is shown in Fig. 1a. It comprises two symmetrical planes: OC is the canyon center line and OD is the maximum slope line between one side of the slope and the horizontal ground (point D may be on AB or BC). The symmetric canyon is controlled by two characteristic slope angles: the central slope angle α and the lateral slope angle δ . α represents the angle between the canyon center line (OC) and the horizontal ground. By contrast, δ represents the angle between the canyon bottom edge (OA) and the horizontal bottom edge (OA'). The angles α and δ determine the geometric structure of the canyon. Additionally, there are two characteristic angles: the maximum slope angle θ and the angle ψ between the center line (OC) and the maximum slope line (OD). According to Viegas and Pita (2004) and Xie et al. (2020), θ and ψ can be calculated using α and δ , and the expression is as follows:

$$\tan \theta = \frac{\sqrt{\tan^2 \alpha + \sin^2 \alpha}}{\cos \alpha} = \frac{\sqrt{\sin^2 \alpha + \tan^2 \alpha}}{\cos \alpha}$$
(1)
$$\tan \psi = \frac{\sin \beta}{\sin \alpha} = \frac{\sin \delta}{\tan \alpha}$$
(2)

$$\tan \psi = \frac{\sin \beta}{\sin \alpha} = \frac{\sin \delta}{\tan \alpha} \tag{2}$$

It can be seen from the expression that θ increases with increase in the central slope angle α and the side slope

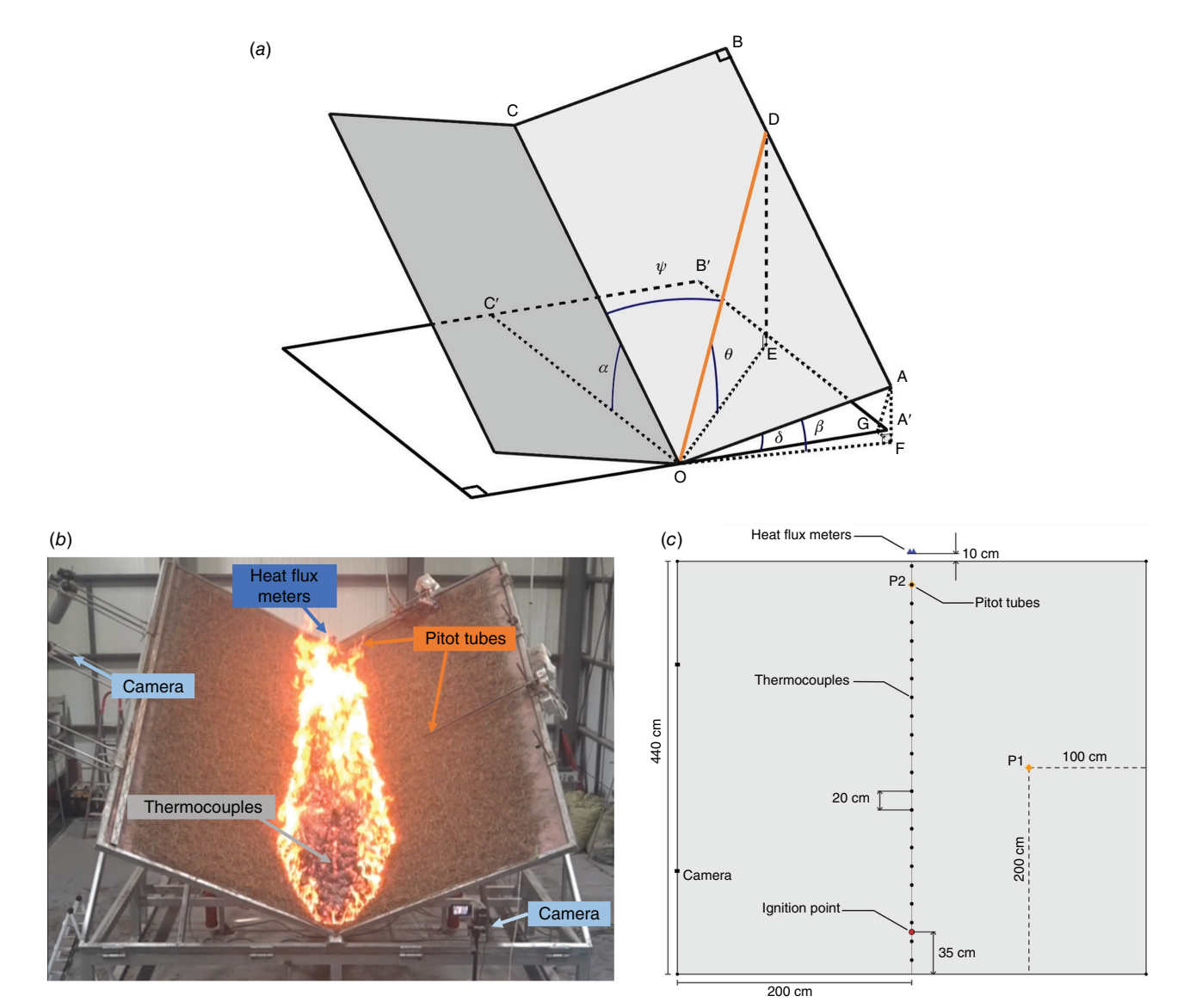


Fig. 1. Geometric structure of symmetric canyon (a); experimental set-up (b); and schematic diagram (c).

angle δ ($\theta > \alpha$ and $\theta \ge \delta$); ψ decreases with increase in α and increases with increase in δ .

Experimental setup

As shown in Fig. 1b, all the experiments were conducted on a 4.4 m (length) \times 4.0 m (width) canyon combustion table in the Wildland Fire Behavior Research Laboratory of Northeast Forestry University. Dead Pinus koraiensis needles were used as fuel (average density, 378 kg m⁻³; average particle diameter, 1483 mm and average surface ratio, 4047 m^{-1}) with a loading capacity of 0.6 kg m⁻² (dry basis) (Viegas and Pita 2004; Xie et al. 2020). The fuel moisture content (FMC) considerably influences fire behavior. After collecting the fuel, it was stored in a warehouse and dried in the shade. The FMC ranged from 8.7 to 13.5%. During the fuel bed preparation stage, a rapid moisture analyzer (A&D ML50) was used to measure the FMC multiple times to ensure stability, with changes not exceeding $\pm 0.5\%$ per experiment. After evenly laying the fuel on the test table, five points were randomly selected to measure the fuel bed depth, at an average depth of 4 cm (average bulk density of the fuel bed, 15 kg m⁻³). The experimental period was mainly concentrated in July and August. The laboratory's ambient temperature was ~25°C, with a relative humidity of ~63%. To ensure accurate results, following previous reports (Viegas and Pita 2004; Xie et al. 2020), we set eight gradients for α , which were 0, 10, 15, 20, 25, 27.5, 30 and 40°, and five gradients for δ , which were 10, 20, 30, 35 and 40°. Among these, $\alpha = 27.5^{\circ}$ was set based on experimental results (when $\alpha = 25^{\circ}$, no eruptive fire occurs) to explore the critical conditions for eruptive fire; hence, only experiments with $\delta = 10, 20$ and 30° were performed. To simplify the naming of different configurations, we use the following explicit form: $[C(\alpha_{\delta})]$, for example, for $\alpha = 0^{\circ}$ and $\delta = 30^{\circ}$, was named C0_30 and for $\alpha = 27.5^{\circ}$ and $\delta = 35^{\circ}$, C27.5_30. To ensure good reproducibility, the test for each configuration was repeated at least once. Each test was ignited by a small cotton ball soaked in alcohol at a distance of 35 cm from the bottom of the canyon center line. Simultaneously, a horizontal fuel bed of 1×1 m was prepared. Under the same conditions, a reference test was performed from the bottom of one side to measure the basic spread speed R_0 under the conditions of no wind and no slope.

On the central line of the canyon, K-type thermocouples (bead diameter 0.2 mm) were installed 8 cm above the surface of the fuel bed, with a constant spacing of 20 cm, sorted from bottom to top, as shown in Fig. 1c. To ensure data accuracy, all thermocouples were calibrated in boiling water prior to the experiments, and the measured error was within \pm 3%. In the experiment, the position of the fire front was determined by identifying the time when the temperature of the thermocouple reached 350°C (Liu *et al.* 2014; Raposo *et al.* 2018). The ignition point was located between the second and third thermocouples. To avoid the influence of residual cotton balls after ignition, the time when the fire front reached the third

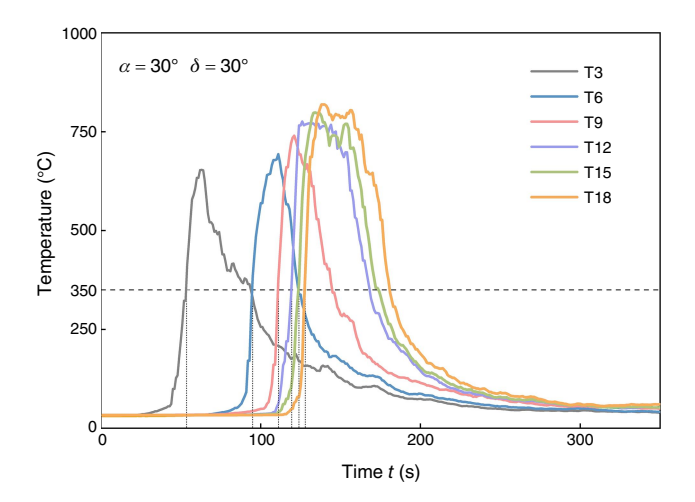


Fig. 2. Typical temperature curve in the experiments ($\alpha=30^\circ$, $\delta=30^\circ$). The number following 'T' indicates the sequential position of the thermocouple.

thermocouple was considered the initial test time, recorded as 0 s. A typical temperature curve measured during an experiment is shown in Fig. 2. Two calibrated bidirectional S-type Pitot tubes (Dwyer Instruments Inc., 160S Series) were connected to the pressure difference meter through hoses and placed at the center of the right plane and the center line near the top of the fuel bed, respectively. The height from the surface of the fuel bed was 15 cm, the Pitot tubes were denoted P1 and P2, and the corresponding measured flow velocities were U1 and U2, respectively. A thermocouple was placed at the measuring position to measure the air temperature, which was used to calculate convection velocity. A total heat flux meter of water-cooled type (Shanghai Anyi Scientific Instrument Co., Ltd, SWT-25-50-WF; range, 0-50 kW m⁻²; response, 2.262 kW m⁻² mV⁻¹; viewing angle, 180°) and a radiative heat flux meter (Shanghai Anyi Scientific Instrument Co., Ltd, SWT-25-50-RWF; range, 0-50 kW m⁻²; response, $3.327 \text{ kW m}^{-2} \text{ mV}^{-1}$; viewing angle, 150°) were placed close at a distance of 10 cm from the top of the fuel bed in the direction of the center line to measure the heat flux density. The sensor window was above and parallel to the surface of the fuel bed. All data were collected at a sampling frequency of 10 Hz. A digital video camera (Sony FDR-AX60, 30 Hz) recorded the experimental process from the front and side of the fuel bed. To better extract data on the evolution of the fire line and avoid the occlusion of smoke and flame plumes, an infrared camera (FLIR T865, resolution 640 × 480 pixels) was used to record and extract the fire line. The infrared camera's measurement temperature range was 300-1500°C.

Data processing

Fire line contour

The sequences of images recorded by the infrared camera were analyzed using the software 'Fire ROS Calculator'. The software calibrated the parameters of the camera by calibrating the object and then used the generated calibration matrix to convert the pixel coordinates in the image into real-world coordinates. This process determines the position of the fire front and extracts the fire line contour, which can yield ROS measurement along the user-defined direction (Abouali and Viegas 2019). The verification results revealed that the software's output error was $\pm 5\%$. This software has been applied in numerous special terrain fire behavior studies (Abouali et al. 2018, 2021; Viegas et al. 2021a; Rodrigues et al. 2023).

ROS

To minimize the impact of external environmental and fuel conditions on fire spread, the experimental results are better compared by studying the internal dynamics of fire spread (Xie *et al.* 2020; Abouali *et al.* 2021; Ribeiro *et al.* 2023). We use the dimensionless ROS R', and the formula used was as follows:

$$R' = \frac{R}{R_0},\tag{3}$$

where R' is the dimensionless ROS, R is the measured ROS in the central line direction and R_0 is the basic ROS under no wind and no slope conditions.

Previous studies have suggested that when R' is ≤ 2 , the ROS is relatively low and approximates a stable spread, but if R' is >5 or increases rapidly in one direction (>5 units min⁻¹), then extreme fire behavior can be considered to be occurring (Viegas and Simeoni 2011; Abouali *et al.* 2018; Rodrigues *et al.* 2019).

Results and analysis

Fire line evolution

Terrain conditions significantly impact fire line evolution, with four different fire line evolution modes being observed under different terrains. Fig. 3 shows the typical canyon fire line evolution under different terrain conditions.

Mode 1

The fire line contour is approximately circular or elliptical. For high δ configurations ($\geq 30^{\circ}$), distinct fire heads appear, and their direction is consistent with the maximum slope line, whereas no fire head appears under other conditions. The evolution of the fire line is similar to the spread of ordinary upslope fires. The fire head first reaches the edges on both sides of the canyon and then spreads upward along the *Y*-axis (vertical direction) in the form of an elliptical arc through the center line. The intersection of the arc and the center line is located at the forefront of the fire line until the top of the fuel bed.

Mode 2

The fire line contour is approximately circular at the beginning, subsequently becoming an isosceles trapezoid

symmetrical about the center line. The direction of the two lateral fire heads is consistent with the direction of the maximum slope line, and in the direction of the Y-axis, the two lateral fire heads connect, forming a broad, straight line of fire approximately perpendicular to the center line in the middle area. The fire head first reaches the edges on both sides of the canyon and then keeps spreading upward, perpendicular to the central line.

Mode 3

The fire line contour is approximately elliptical at the beginning (the long axis is located at the center line), thereafter forming a butterfly shape symmetrical about the center line. This contour is completely different from the ordinary upslope fire. The direction of the two lateral fire heads deviates from the maximum slope line from observation and moves closer to the center line. Along the *Y*-axis direction, the ROS at the center line is slightly lower than that of the two lateral fire heads, forming two elliptical arcs symmetrical about the center line.

Mode 4

The fire line contour is also approximately elliptical (the long axis is at the center line) at the initial stage. Subsequently, a single fire head forms near the center line and spreads upward until the top of the fuel bed. With increase in α and δ , the time required for the fire to spread to the top decreases, the fastest time being $\sim\!60$ s. Subsequently, two symmetrical linear fire lines form to connect the bottom and the top, spreading laterally (in the *X*-axis direction) to both sides. The fire head in this mode completely deviates from the maximum slope line, forming a single fire head near the center line.

The parameters α and δ , which control the terrain structure of the canyon, significantly affect the evolution of the fire line. $\alpha=0^\circ$ forms a unique configuration with a ψ angle of 90° . The maximum slope line is perpendicular to the center line, and the fire line spreads along it. When δ is fixed and α increases, the angle of the fire head direction deviating from the maximum slope line gradually increases until a single fire head forms near the center line. When α is fixed and δ increases, the angle between the fire head and the center line gradually increases (except for $\alpha=0^\circ$ and 40°) until the fire head direction aligns with the maximum slope line. The figure clearly shows that the fire line evolution mode changes more significantly with the angle of α . Therefore, it can be considered that the influence of α on fire line evolution is more significant than that of δ .

Viegas and Pita (2004) proposed an analytical model based on the spread of ordinary upslope fire. They assumed that in the absence of wind, the fire would spread like a single ellipse or a double ellipse, with its central axis consistent with the direction of the maximum slope line. Our results show that only in Mode 1 is the fire line evolution similar to the results of the analytical model, with differences in other modes. Particularly in Mode 3 and Mode 4, the fire head deviates

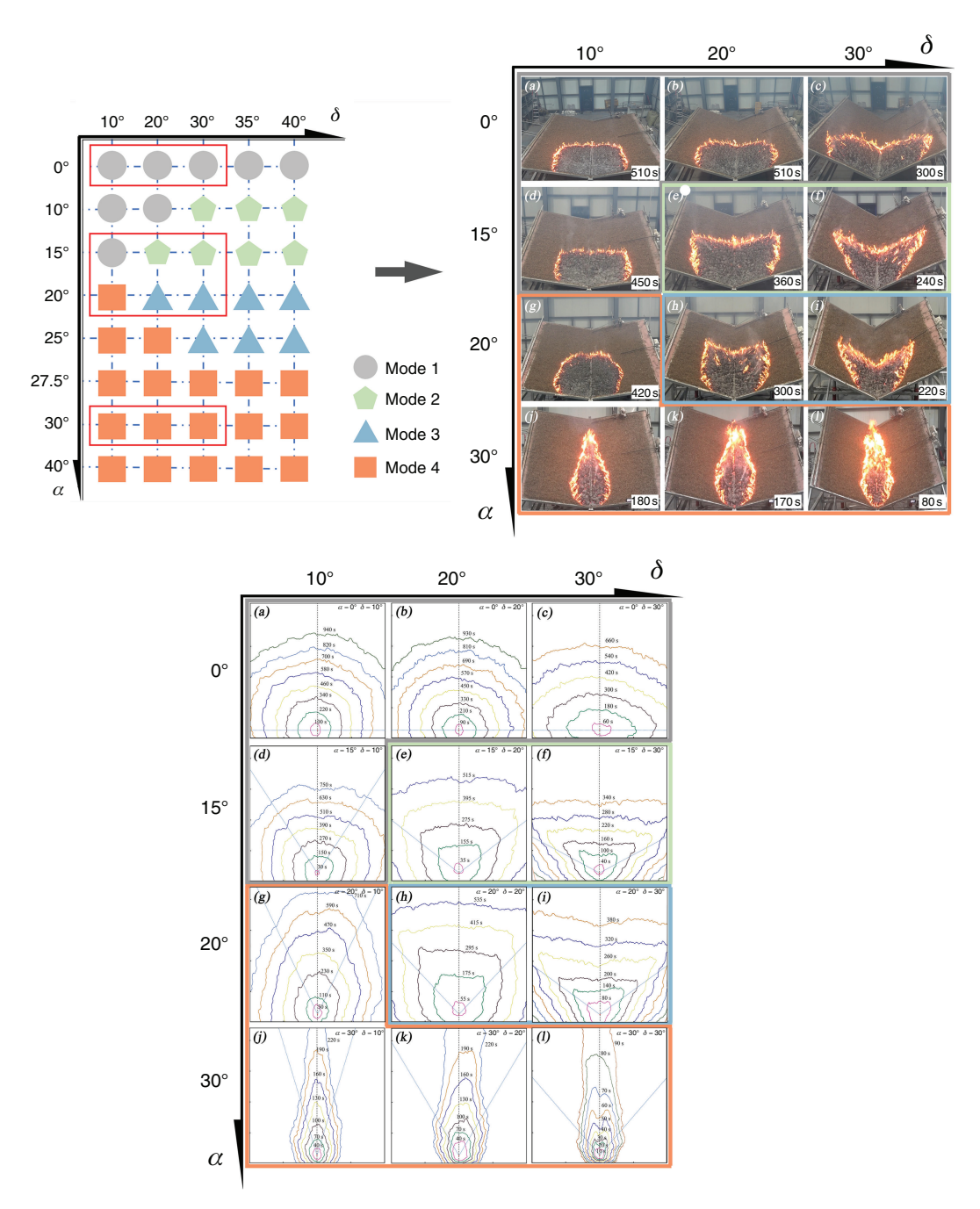


Fig. 3. The fire line contours under different terrains. The (a-c) $\alpha = 0^\circ$; (d-f) $\alpha = 15^\circ$, (g-i) $\alpha = 20^\circ$ and (j-l) $\alpha = 30^\circ$. The blue dotted line in the figure represents the maximum slope line.

from the maximum slope line, moves closer to the center line and even forms a single fire head near the center line. According to experimental data and theoretical analysis, Xie *et al.* (2020) proved that there was an interaction between the two lateral fire fronts, which affected the preheating mechanism for unburned fuels in front of the fire front, resulting in deflection of the fire line and affecting the ROS. For two parallel rectangular flames, the interaction of the fires depends on the distance between the flames, the size

of the fuel bed and the heat release rate (Liu *et al.* 2019). The smaller the distance between the fires, the stronger the interaction. As α increases, the maximum slope line moves to the center line, causing the theoretical maximum spread velocity direction to move to the central line. This movement decreases the distance between the two lateral fire fronts, making their interaction more pronounced and increasing the angle of fire head direction deflection (Maynard *et al.* 2016; Raposo *et al.* 2018; Liu *et al.* 2019; Xie *et al.* 2020).

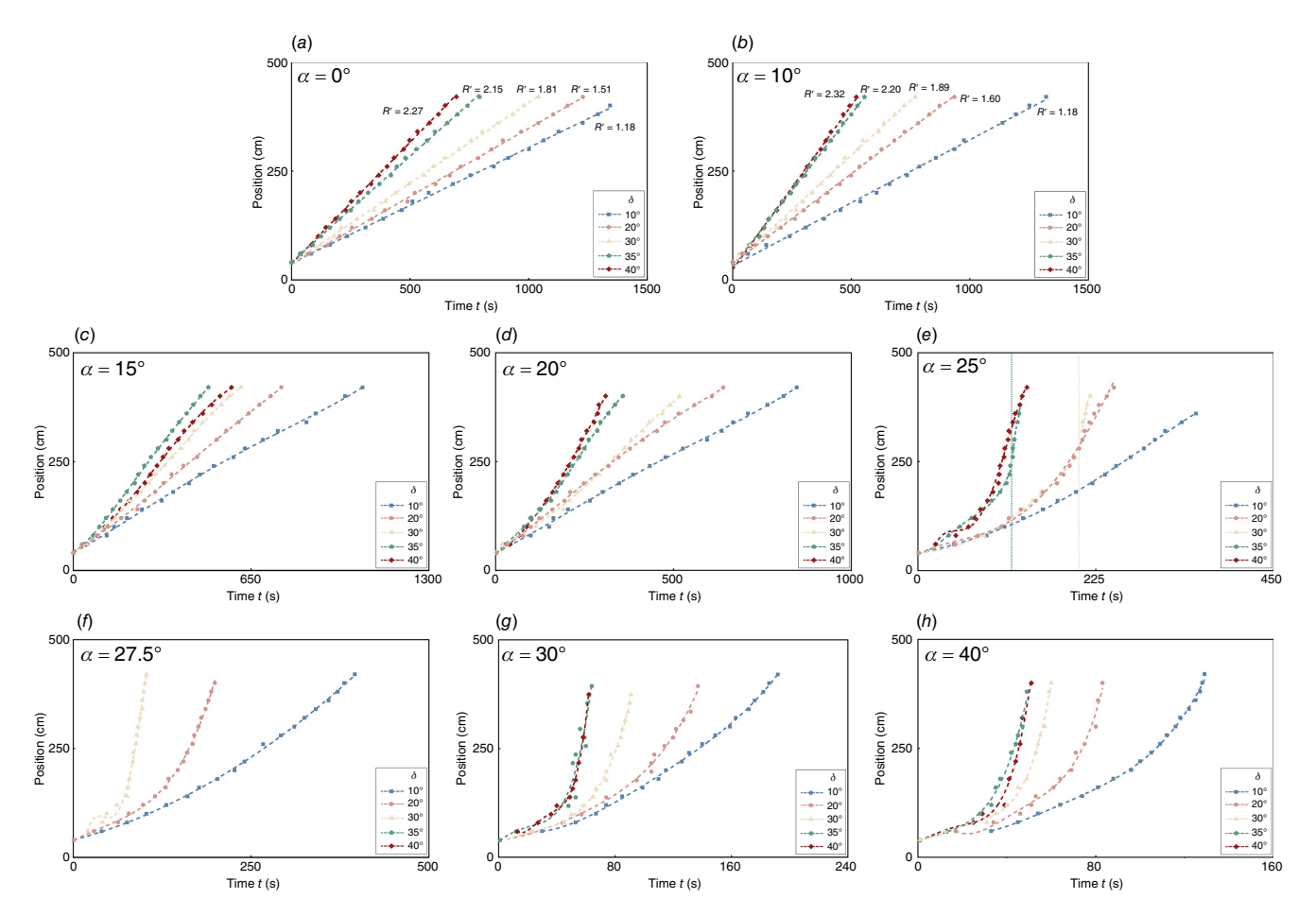


Fig. 4. Position of the fire front in the experiment (along the center line of the canyon). The (a-h) correspond to α of 0°, 10°,15°, 20°, 25°, 27.5°, 30°, and 40°, respectively.

As δ increases, although the theoretical angle between the fire head direction and the center line increases, the distance between the two planes of the canyon decreases, enhancing the interaction.

Rate of spread

Canyon fire spread is a dynamic process, and ordinary linear regression cannot reflect the change in ROS with time. Therefore, we performed a polynomial regression on the position and time of the fire front arrival (Xie *et al.* 2020) and then obtained the spread speed (R) by deriving different positions of the fitting curve and calculating the dimensionless spread speed (R). The position and time of the fire front are shown in Fig. 4, and the dashed line represents the fitting curve. For configurations with $\alpha = 0^{\circ}$ and 10° , the difference in ROS is not significant owing to the small α . The value of R' obtained is <2.5, with a variation range within 0.5. This indicates that the spread speed is stable; hence, R' is obtained via linear fitting. Additionally, for C25_30 and C25_35, owing to the fire line evolution, there is a brief, sudden acceleration in their spread, and the polynomial regression performs poorly.

Therefore, a piecewise regression method was used to improve the accuracy of the ROS calculation.

Fig. 5 shows the dimensionless ROS (R') under different terrain conditions. When α is $\geq 15^{\circ}$, R' begins to exhibit dynamic characteristics. This results from the interaction between the fire and its surrounding environment, with the characteristics of fire behavior changing over time even without changes in external conditions (Viegas et al. 2021b, 2022). Under different terrain conditions, R' shows different modes. For low slope conditions of $\alpha = 15^{\circ}$ and 20° and $\delta = 10^{\circ}$ and 20° (Fig. 5a, b), the value of R' fluctuates around 2, but the range of variation does not exceed 1, which is similar to stable spread (Wang et al. 2024). For other configurations of $\alpha = 15^{\circ}$ and 20° , all configurations of $\alpha = 25^{\circ}$ and C27.5_10 (Fig. 5a-d), the dynamic characteristics of the R' are more pronounced, and the acceleration of R' decreases over time. When R' reaches its peak, it gradually decreases to approach the initial R' or another stable value. In the two modes described above (Fig. 5a-d), R' does not exhibit growth; hence, its final trend is either declining or remaining stable. However, for C27.5_20, C27.5_30 and all configurations of $\alpha = 30^{\circ}$ and

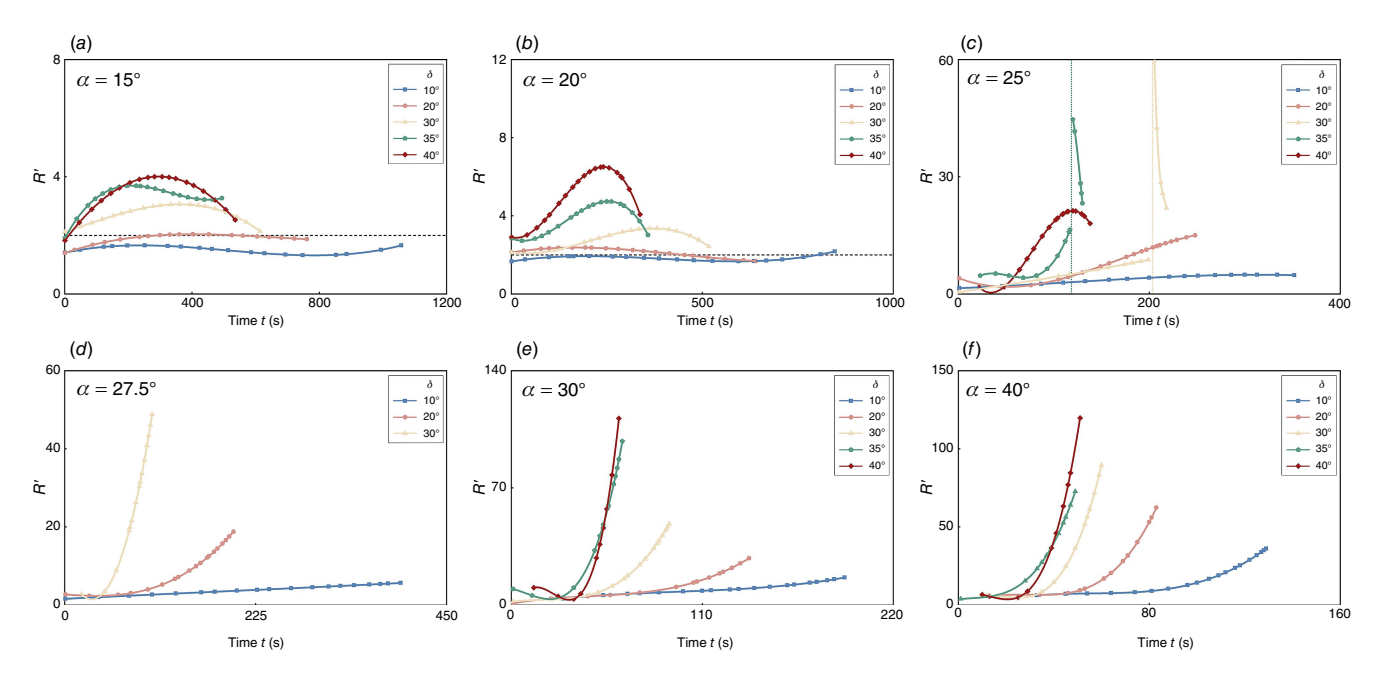


Fig. 5. Dimensionless rate of spread, R'. The horizontal lines in (a) and (b) indicate the value corresponding to R' = 2. The (a–f) correspond to α of 15°, 20°, 25°, 27.5°, 30°, and 40°, respectively.

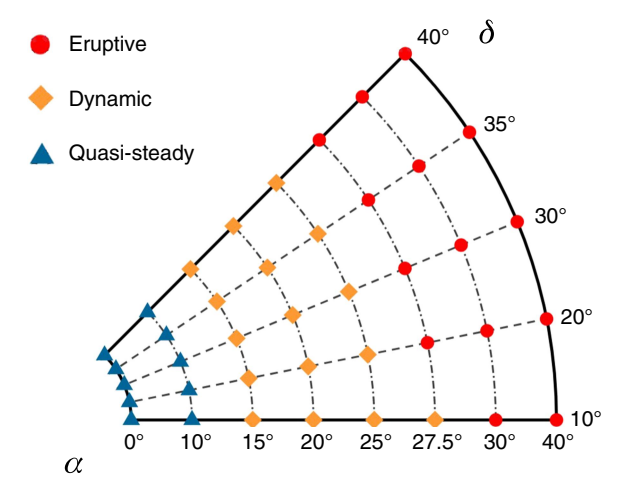


Fig. 6. Occurrence of eruptive fire in a canyon under different experimental conditions.

40° (Fig. 5*d*–*f*), after an initial phase of relatively stable spread, acceleration continuously increases, and the ROS demonstrates an exponential growth trend, consistent with the characteristics of eruptive fires (Viegas and Simeoni 2011; Liu 2023). This indicates that eruptive fire occurred under those terrain conditions. Our results show that the critical conditions for the eruptive fire in the canyon are $\alpha = 27.5^{\circ}$, $\delta = 20^{\circ}$ (C27.5_20), as shown in Fig. 6. When α is $\geq 30^{\circ}$ or $\alpha = 27.5^{\circ}$ and δ is $\geq 20^{\circ}$, eruptive fire occurs in the canyon. In our experiment, R' increases monotonically with α and δ . For δ increasing from 30° to 40°, no decrease in R' is observed, as mentioned by Viegas and Pita (2004), possibly because of spatial constraints. When α is $\geq 30^{\circ}$,

eruptive fire can occur even when $\delta=10^\circ$. This suggests that the occurrence of eruptive fire is more dependent on α than on δ , and α has a more significant impact on R'. The trench configuration can be regarded as an analog of confined slopes in canyons (Liu *et al.* 2023). Previous studies on trench fires indicate a critical slope for eruptive fires related to the height (aspect ratio) of the trench walls (Xie *et al.* 2017). This is consistent with our results. Specifically, when $\alpha=27.5^\circ$, the ROS tends to stabilize at $\delta=10^\circ$, whereas an increase in δ to 20° leads to an exponential rise in the ROS, indicating the occurrence of eruptive fire.

Heat flux

To analyze the heat transfer mechanism of canyon fire spread, we measured the total and radiative heat flux at the top of the center line. The measured heat flux data showed noticeable fluctuations over time. We used the method of Liu et al. (2014, 2015) and applied the Fourier low-pass filtering algorithm with a cut-off frequency of 0.1 Hz to smooth the heat flux data, with the peak remaining almost unchanged after treatment. Fig. 7 shows the heat flux data under typical configurations. The total heat flux and the radiative heat flux increase with the characteristic slope angles α and δ . Previous studies have shown that the sudden fire acceleration of eruptive fires often involves a significant increase of convective heating (Viegas and Pita 2004; Dold and Zinoviev 2009; Xie et al. 2017; Liu 2023). Our results showed that for configurations where eruptive fires did not occur (Fig. 6), the total heat flux and radiative heat flux were approximately the same, indicating that

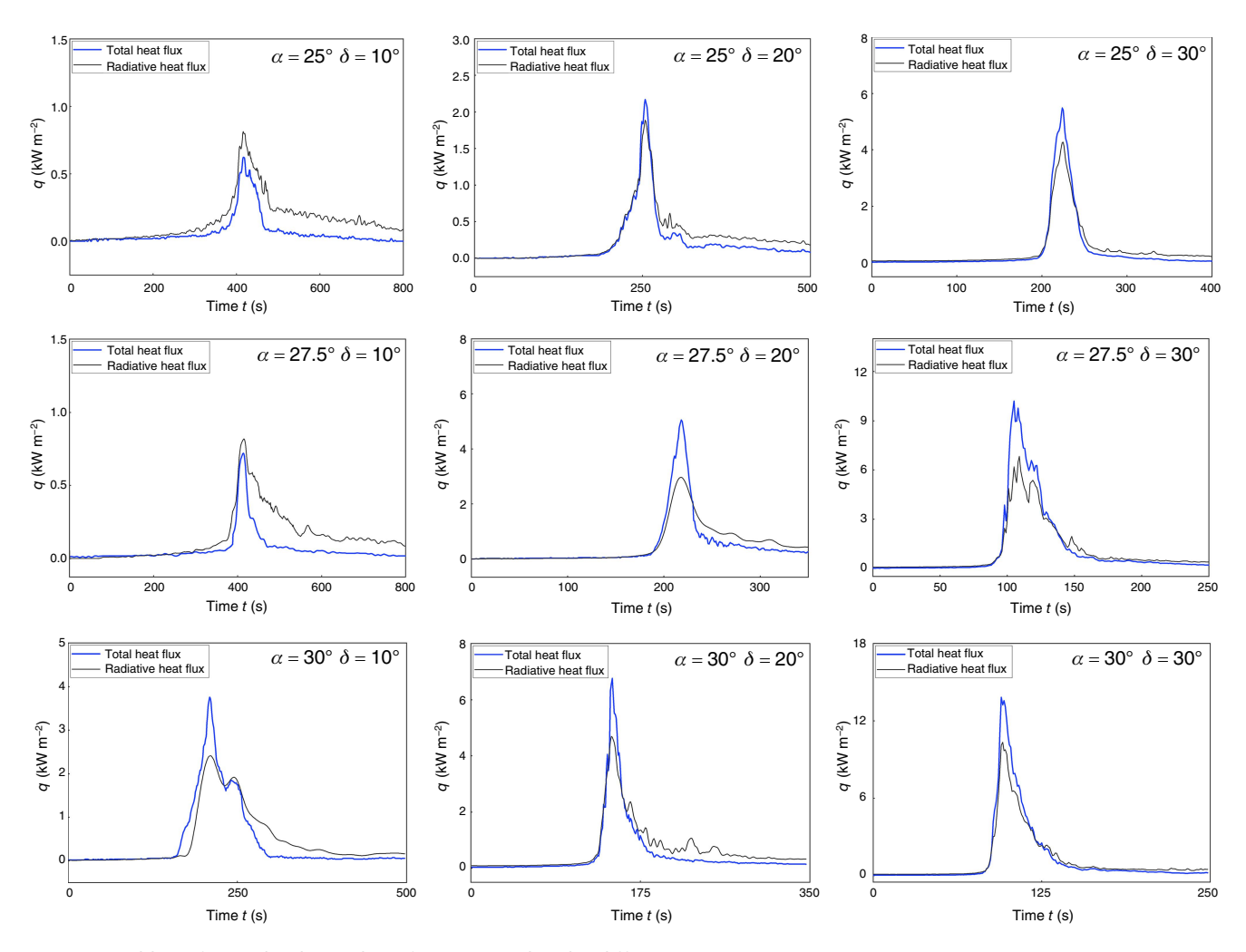


Fig. 7. Total heat flux and radiation heat flux measured under different terrains.

radiative heating is the primary mechanism of fire spread, and convective heating does not exist or is not obvious. For configurations with α of $\geq 30^{\circ}$ or $\alpha = 27.5^{\circ}$, δ of $\geq 20^{\circ}$, where eruptive fires occurred (Fig. 6), the total heat flux was significantly greater than the radiant heat flux, indicating a significant increase in convective heating. Convective heating and radiative heating jointly dominated in the preheating of unburned fuels in front of the fire front, resulting in a sharp increase in R'.

Flow velocity

The flow velocities of typical configurations are shown in Fig. 8. The upslope direction along the center line is positive, and the dotted line in the figure represents the fire front arrival time. Initially, the flow velocity fluctuates around 0. As the fire front approaches the Pitot tube, the flow velocity decreases and then rapidly increases. This rapid increase in flow velocity is caused by the upslope wind induced by the fire (Liu 2023). When the Pitot tube is within the fire front, the peak is reached. After the fire

front passes, the flow velocity remains positive for some time and then gradually decreases. In all experiments, the flow velocity increased with increase in α and δ , while the time required to reach the peak velocity decreased with the increase in slope. This is because the canyon shape influences both fire interactions and air entrainment. First, as α and δ increase, the interaction between fire fronts becomes more intense, promoting combustion, strengthening fireinduced flow and resulting in higher flow velocities. Second, α and δ also affect air entrainment. An increase in α enlarges the inflow gap between the front and rear of the fire front and reduces the flame tilt angle, resulting in a higher velocity component along the upslope direction. An increase in δ increases the restriction on lateral air entrainment, thereby contributing to an increase in the flow velocity parallel to the center line.

Viegas and Pita (2004) showed that fire-induced flow plays a vital role in fire acceleration. When the direction of convection in front of the fire front is consistent with the spread speed, it produces a convective heating effect on the unburned fuels in front and increases the ROS of the fire

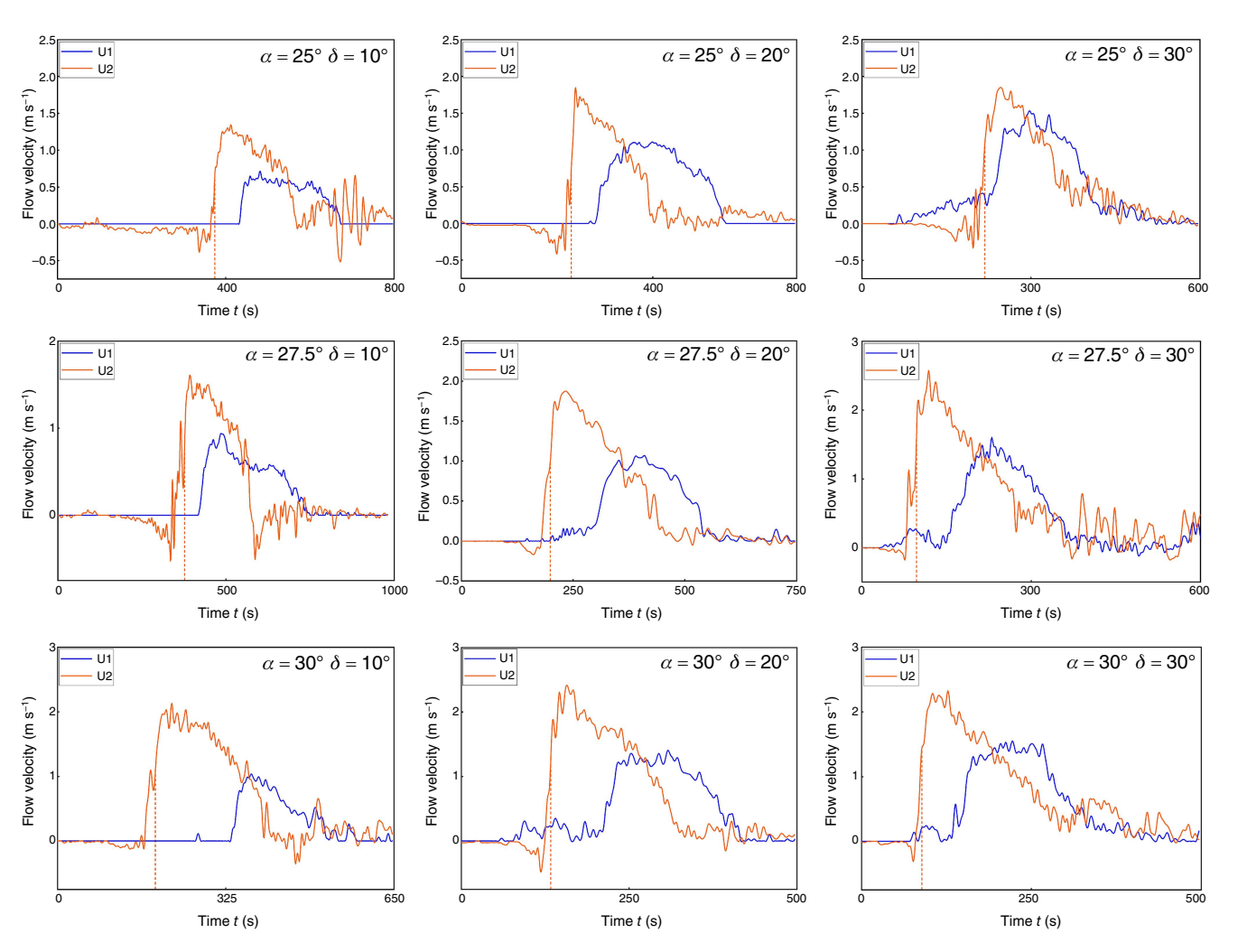


Fig. 8. Flow velocity measured under different terrains. U1 and U2 were measured at P1 (the right plane center) and P2 (above the center line of the fuel bed), respectively.

front (Dold and Zinoviev 2009). The strength of convective heating is related to the positive flow velocity before the fire front reaches the fuel (Xie *et al.* 2017). Fig. 8 shows the flow velocity of the fire front when it reaches the Pitot tube (P2). The results show that the flow velocity at the time of fire front arrival increase with increase in α and δ , especially in the configurations where eruptive fire occurs. The velocity is significantly higher than that in other configurations, indicating noticeable convective heating (Fig. 9).

The convective heating range refers to a certain spatial extent in front of the fire front where convective heating effects are present. It can be calculated based on the positive convection velocity, the arrival of the fire front at the Pitot tube and the ROS. The results are shown in Fig. 10. As no obvious convective heating was observed under the conditions of no eruptive fire, no calculation was performed. Our results show that the convective heating range increases with α and δ , reaching up to 340 cm. Compared with common upslope fires, eruptive fires significantly enhance

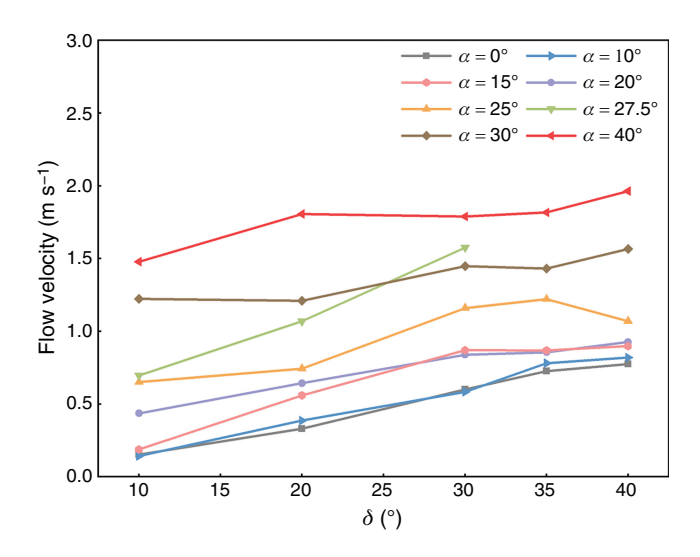


Fig. 9. The flow velocity when the fire front reaches Pitot tube P2.

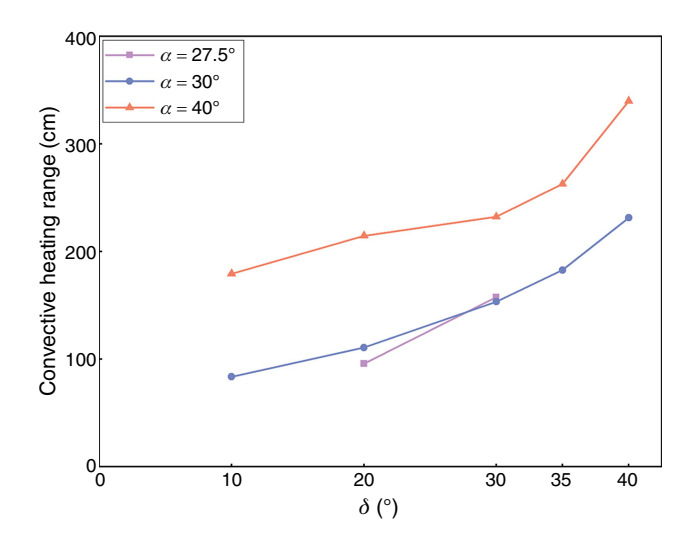


Fig. 10. Convective heating range of eruptive fire.

convective heating and expand their range, preheating the fuel together with radiation heating (Liu *et al.* 2014, 2015, 2023; Xie *et al.* 2017). This significant convective heating plays an essential role in preheating fuel, resulting in a sharp increase in ROS, which is the basic mechanism of eruptive fire in a canyon (Dold and Zinoviev 2009; Xie *et al.* 2020).

Overall, canyons are hazardous terrains where, under certain slopes, interactions between a fire and the surrounding environment can induce eruptive fire even when external conditions remain unchanged. When eruptive fire occurs in a canyon, fire behavior changes obviously, with convective heating ahead of the fire front significantly enhanced, resulting in a sharp increase in the ROS along the center line. It also alters the fire line evolution: regardless of changes in slope, the fire head consistently deviates completely from the maximum slope line, forming a single head near the center line that rapidly spreads upslope. Additionally, convective heating can occur over long distances, necessitating vigilance from firefighters. To better understand canyon fire spread, further experiments are warranted to explore the physical processes involved considering external wind, fuel type and load, and other conditions. Field-scale experiments should be conducted to avoid scale effects and verify the current experimental and analytical results.

Conclusion

Herein, a series of fire spread experiments using dead pine needle fuel beds was conducted on symmetrical canyons under different terrain conditions. The variation of canyon fire spread with terrain was systematically analyzed, the critical conditions for eruptive fire were obtained and the heat transfer mechanism was studied. The main conclusions are as follows.

(1) Terrain strongly influences the fire line evolution of canyon fires, and four different evolution modes were

identified. As α increases, the angle of the fire head deviating from the maximum slope line gradually increases, moving to the center line and eventually forming a single fire head near the center line. In addition to $\alpha=0^\circ$ 40°, increase in δ leads to a greater angle between the fire head direction and the center line. The influence of α on the fire line evolution is more pronounced. This deflection of the fire head is caused by the interaction between the two lateral fire fronts.

- (2) For ROS along the center line, three different change patterns were identified under different terrains. ROS increased with α and δ . When α was $\geq 15^{\circ}$, ROS exhibited dynamic characteristics. In this experiment, $\alpha = 27.5^{\circ}$ and $\delta = 20^{\circ}$ were the critical conditions for eruptive fire in the canyon. When the slope of the canyon reached critical conditions, eruptive fire occurred, and ROS sharply increased.
- (3) For configurations where eruptive fire does not occur, radiation is the main preheating mechanism for unburned fuels, and convection heating is either absent or not apparent. For configurations where eruptive fire occurs, convective heating is significantly enhanced and its influence range also significantly increases, dominating the preheating of fuel together with radiation, eventually resulting in accelerated fire spread. Terrain affects the preheating mechanism ahead of the fire front. As α and δ increase, convective heating gradually increases. This strong convective heating is the basic mechanism of eruptive fire in canyons.

References

Abouali A, Viegas DX (2019) Fire ROS Calculator: a tool to measure the rate of spread of a propagating wildfire in a laboratory setting. Journal of Open Research Software 7, 24. doi:10.5334/jors.221

Abouali A, Raposo JR, Viegas DX (2018) The role of the terrain-modified wind on driving the fire behaviour over hills – an Experimental and Numerical Analysis. In 'Proceedings of the 8th International Conference on Forest Fire Research', 9–16 November 2018. pp. 677–694. (Coimbra, Portugal) doi:10.14195/978-989-26-16-506 75

Abouali A, Viegas DX, Raposo JR (2021) Analysis of the wind flow and fire spread dynamics over a sloped ridgeline hill. *Combustion and Flame* **234**, 111724. doi:10.1016/j.combustflame.2021.111724

Balbi J-H, Chatelon FJ, Rossi JL, Simeoni A, Viegas DX, Rossa C (2014) Modelling of eruptive fire occurrence and behaviour. *Journal of Environmental Science and Engineering B* 3, 115–132.

Chatelon FJ, Balbi JH, Rossi JL, Filippi JB, Marcelli T, Rossa C, Viegas DX (2011) The Importance of Fire Front Width in the Anticipation of Eruptive Fires. In 'Proceedings of the Seventh Mediterranean Combustion Symposium', 11–15 September 2011. (Chia Laguna, Cagliari)

Dold JW, Zinoviev A (2009) Fire eruption through intensity and spread rate interaction mediated by flow attachment. *Combustion Theory and Modelling* **13**, 763–793. doi:10.1080/13647830902977570

Dold JW, Zinoviev A (2011) Intensity accumulation in unsteady firelines: a simple model for vegetation engagement. *Fire Safety Journal* **46**, 63–9. doi:10.1016/j.firesaf.2010.12.001

Duane A, Castellnou M, Brotons L (2021) Towards a comprehensive look at global drivers of novel extreme wildfire events. *Climatic Change* **165**, 43. doi:10.1007/s10584-021-03066-4

Liu N (2023) Wildland surface fire spread: mechanism transformation and behavior transition. Fire Safety Journal 141, 103974. doi:10.1016/j. firesaf.2023.103974

- Liu N, Wu J, Chen H, Xie X, Zhang L, Yao B, Zhu J, Shan Y (2014) Effect of slope on spread of a linear flame front over a pine needle fuel bed: experiments and modelling. *International Journal of Wildland Fire* **23**, 1087–1096. doi:10.1071/WF12189
- Liu N, Wu J, Chen H, Zhang L, Deng Z, Satoh K, Viegas DX, Raposo JR (2015) Upslope spread of a linear flame front over a pine needle fuel bed: the role of convection cooling. *Proceedings of the Combustion Institute* **35**, 2691–2698, doi:10.1016/J.PROCI.2014.05.100
- Liu N, Zhang S, Luo X, Lei J, Chen H, Xie X, Zhang L, Tu R (2019) Interaction of two parallel rectangular fires. *Proceedings of the Combustion Institute* 37, 3833–3841. doi:10.1016/j.proci.2018.06.158
- Liu N, Lei J, Gao W, Chen HX, Xie XD (2021) Combustion dynamics of large-scale wildfires. *Proceedings of the Combustion Institute* **38**, 157–198. doi:10.1016/j.proci.2020.11.006
- Liu N, Yuan X, Xie X, Lei J, Gao W, Chen H, Zhang L, Li H, He Q, Korobeinichev O (2023) An experimental study on mechanism of eruptive fire. Combustion Science and Technology 195, 3168–3180. doi: 10.1080/00102202.2021.2019240
- Lopes AMG, Sousa ACM, Viegas DX (1995) Numerical simulation of turbulent flow and fire propagation in complex topography. *Numerical Heat Transfer Part A* 27, 229–253. doi:10.1080/10407789508913698
- Maynard T, Princevac M, Weise DR (2016) A study of the flow field surrounding interacting line fires. *Journal of Combustion* 1, 6927482. doi:10.1155/2016/6927482
- Pimont F, Dupuy J-L, Linn RR (2012) Coupled slope and wind effects on fire spread with influences of fire size: a numerical study using FIRETEC. *International Journal of Wildland Fire* **21**, 828–842. doi:10.1071/WF11122
- Raposo JR, Viegas DX, Xie X, Almeida M, Figueiredo A, Porto L, Sharples J (2018) Analysis of the physical processes associated with junction fires at laboratory and field scales. *International Journal of Wildland Fire* 27, 52–68. doi:10.1071/WF16173
- Ribeiro C, Viegas DX, Raposo J, Reis L, Sharples J (2023) Slope effect on junction fire with two non-symmetric fire fronts. *International Journal of Wildland Fire* **32**, 328–335. doi:10.1071/WF22152
- Rodrigues A, Ribeiro C, Raposo J, Viegas DX, André J (2019) Effect of canyons on a fire propagating laterally over slopes. *Frontiers of Mechanical Engineering* 5, 402–409. doi:10.3389/fmech.2019.00041
- Rodrigues A, Viegas DX, Almeida M, Ribeiro C, Raposo J, André J (2023) Fire propagating laterally over a slope with and without an embedded canyon. *Fire Safety Journal* **138**, 103791. doi:10.1016/j. firesaf.2023.103791
- Rothermel RC (1972) A mathematical model for predicting fire spread in wildland fuels. Research Paper INT-115. (USDA Forest Service, Intermountain Forest and Range Experiment Station)

- Silvani X, Morandini F, Dupuy J-L (2012) Effects of slope on fire spread observed through video images and multiple-point thermal measurements. *Experimental Thermal and Fluid Science* **41**, 99–111. doi:10.1016/j.expthermflusci.2012.03.021
- Silvani X, Morandini F, Dupuy JL, Susset A, Vernet R, Lambert O (2018) Measuring velocity field and heat transfer during natural fire spread over large inclinable bench. *Experimental Thermal and Fluid Science* **92**, 184–201. doi:10.1016/J.EXPTHERMFLUSCI.2017.11.020
- Viegas DX (2004) A mathematical model for forest fire blow-up. Combustion Science and Technology 177, 27–51. doi:10.1080/00102200590883624
- Viegas DX (2006) Parametric study of an eruptive fire behaviour model. *International Journal of Wildland Fire* **15**, 169–177. doi:10.1071/WF05050
- Viegas DX, Pita LP (2004) Fire spread in canyons. *International Journal of Wildland Fire* 13, 253–274. doi:10.1071/WF03050
- Viegas DX, Simeoni A (2011) Eruptive behaviour of forest fires. Fire Technology 47, 303–320. doi:10.1007/s10694-010-0193-6
- Viegas DX, Ribeiro LM, Viegas MT, Pita LP, Rossa C (2009) Impacts of fire on society: extreme fire propagation issues. In 'Earth Observation of Wildland Fires in Mediterranean Ecosystems'. (Ed. E Chuvieco) pp. 97–109. (Springer: Berlin, Germany)
- Viegas DX, Rodrigues A, Abouali A, Almeida M, Raposo J (2021a) Fire downwind a flat surface entering a canyon by lateral spread. Fire Safety Journal 122, 103349. doi:10.1016/j.firesaf.2021.103349
- Viegas DXFC, Raposo JRN, Ribeiro CFM, Reis LCD, Abouali A, Viegas CXP (2021b) On the non-monotonic behaviour of fire spread. *International Journal of Wildland Fire* **30**, 702–719. doi:10.1071/WF21016
- Viegas DXFC, Raposo JRN, Ribeiro CFM, Reis L, Abouali A, Ribeiro LM, Viegas CXP (2022) On the intermittent nature of forest fire spread Part 2. International Journal of Wildland Fire 31, 967–981. doi:10.1071/WF21098
- Wadhwani R, Sutherland D, Moinuddin K, Huang X (2023) Numerical simulation of two parallel merging wildfires. *International Journal of Wildland Fire* **32**, 1726–1740. doi:10.1071/WF23071
- Wang S, Thomsen M, Huang X, Fernandez-Pello C (2024) Spot ignition of a wildland fire and its transition to propagation. *International Journal of Wildland Fire* **33**, WF23207. doi:10.1016/j.csite.2023.103523
- Xie X, Liu N, Lei J, Shan Y, Zhang L, Chen H, Yuan X, Li H (2017) Upslope fire spread over a pine needle fuel bed in a trench associated with eruptive fire. *Proceedings of the Combustion Institute* **36**, 3037–3044. doi:10.1016/j.proci.2016.07.091
- Xie X, Liu N, Raposo JR, Viegas DX, Yuan X, Tu R (2020) An experimental and analytical investigation of canyon fire spread. *Combustion and Flame* 212, 367–376. doi:10.1016/J.COMBUSTFLAME.2019.11.004

Data availability. The data that support the findings of this study are available from the corresponding author on reasonable request.

Conflicts of interest. The authors declare no conflicts of interest.

Declaration of funding. This work was funded by the National Key Research and Development Program of China (2022YFC3003002), the Key Research and Development Program of Heilongjiang Province (ZZDYF220100001), and the Key Research and Development Program of Heilongjiang Province (ZZDYF250100002).

Acknowledgements. We thank the Northern Forest Fire Management Key Laboratory of State Forestry and Grassland Administration and the National Innovation Alliance of Wildland Fire Prevention and Control Technology of China for supporting this research.

Author affiliation

Akey Laboratory of Sustainable Forest Ecosystem Management – Ministry of Education, Northern Forest Fire Management Key Laboratory of State Forestry and Grassland Administration, College of Forestry, Northeast Forestry University, 26 Hexing Road, Harbin 150040, China.